UNSTEADY FLOW AND HEAT TRANSFER OF MAXWELL NANOFLUID IN A FINITE THIN FILM WITH INTERNAL HEAT GENERATION AND THERMOPHORESIS

by

Tingting LIU[a], Lin LIU[a,b] and Liancun ZHENG[a*]

[a] School of Mathematics and Physics, University of Science and Technology Beijing, Beijing, China
[b] School of Energy and Environmental Engineering, University of Science and Technology Beijing, Beijing, China

Original scientific paper
https://doi.org/10.2298/TSCI170129097L

This paper studies the unsteady flow and heat transfer of Maxwell nanofluid in a finite thin film over a stretching sheet. The heat generation, Brownian motion and thermophoresis are taken into consideration. Coupled non-linear governing PDE are formulated and local similarity solutions are obtained by BVP4C. Results show that, unlike Newtonian fluid, the relaxation characteristics of Maxwell fluid have strongly effects on thermal and concentration transmission, there exist intersections in the distributions of temperature and concentration, the local Nusselt and Sherwood numbers increases with the increase of Brownian number. Moreover, the combined effects of pertinent physical parameters, such as the unsteadiness, Deborah number, Prandtl number, Lewis number, Brownian number, thermophesis parameter, local Nusselt number, and local Sherwood number on velocity, temperature, and concentration fields are also analyzed and discussed.

Key words: *Maxwell nanofluid, unsteady flow, Brownian motion, thermophoresis*

Introduction

The flow and heat transfer within a thin film liquid over an unsteady stretching sheet has acquired special attention due to its widespread technological applications. In particular, it is closely related to the mechanical forming processes, such as wire and fiber coating, melting-spinning, foodstuff processing, and extrusion processing. The most important aim of every extrusion is to keep the surface quality of the extrudation and the flow induced by the stretching motion of a flat elastic sheet. Therefore, it is worthy to analyze the momentum and thermal transports within a thin film liquid film on a continuously stretching surface.

Considering the steady 2-D flow of a Newtonian fluid, Crane [1] studied the fluid flow caused by a stretching sheet continuously moving with a linear velocity variation. Wang [2] applied similarity transformation to reduce the unsteady Navier-Stokes equations and found asymptotic and numerical solutions. Andersson *et al*. [3] investigated the momentum in a thin liquid film of a power-law fluid caused by the unsteady stretching surface. Chen [4] researched the momentum and heat transfer of a power-law fluid film due to the unsteady stretching sheet. Wang [5] analyzed the momentum and heat transfer in a laminar liquid film by using the homotopy analysis method. Dandapat *et al*. [6] analyzed the influence of the thermo-capillarity on the

* Corresponding author, e-mail: liancunzheng@163.com

Newtonian fluid flow within a liquid film on an unsteady stretching sheet. Chen [7] investigated the thermo-capillarity effects of power-law liquids. Abel *et al*. [8] presented a mathematical analysis of MHD flow and heat transfer to a laminar liquid film over an unsteady stretching surface. Abbas *et al*. [9, 10] examined 2-D MHD boundary-layer flow of an upper-convected Maxwell fluid and the flow of a second grade fluid over a stretching sheet. Hayat *et al*. [11] studied the mass transfer of the upper-convected Maxwell fluid past a porous shrinking sheet. Sajid *et al*. [12] researched the unsteady flow of a second grade over a stretching sheet. More references about the flow and heat transfer of Maxwell fluid had been studied in [13-16]. Combined electrical MHD Ohmic dissipation forced and free convection of an incompressible Maxwell fluid on a stagnation point had been studied by Hsiao [17]. Kumaran [18] investigated the MHD Casson and Maxwell flows over a stretching sheet with cross diffusion. More references about the flow and heat transfer of Maxwell nanofluid had been studied in [19, 20].

In recent years, convective heat transfer in nanofluids has received considerable attentions. The word *nanofluid* was coined by Choi [21] who describes a liquid suspension containing ultra-fine particles with typical length on the order of 1-50 nm. Conventional heat transfer fluids, including oil, water, and ethylene glycol mixture are poor heat transfer fluids. The thermal conductivity of these fluids plays an important role on the heat transfer coefficient between the heat transfer medium and surface. Experimental studies [22-24] displayed that the thermal conductivity of the base liquid can be enhanced even with small volumetric fraction of nanoparticles. Khan and Pop [25] considered the laminar fluid-flow of a nanofluid past a stretching sheet. By considering the Brownian diffusion and thermophoresis, the flow in nanofluids had attracted considerable attentions and a good amount of literatures had been generated on this problem [26-31]. Shehzad *et al*. [32] studied the heat and mass transfer characteristics in 3-D flow of an Oldroyd-B fluid. Lin *et al*. [33] researched the flow of MHD pseudo-plastic nanofluid in a finite film over unsteady stretching surface with internal heating. Li *et al*. [34] explored the unsteady MHD flow and radiation heat transfer of nanofluid within a finite thin film over stretching surface. The heat and mass transfer of nanofluid with thermal radiation and chemical reaction can be found in [35-37]. Bhatti *et al*. [38] studied the Titanium magneto-nanoparticles suspended in water-based nanofluid by entropy analysis. Some more studies on the flow of nanofluid through a Riga plate can be found from [39-41]. Hayat *et al*. [42, 43] explored the MHD flow of nanofluid in presence of non-linear thermal radiation and the flow due to a rotating disk with a numerical study.

Motivated by the previous discussions, we analyze the unsteady Maxwell fluid flow and mass transfer in a finite thin film induced by an unsteady stretching sheet. The effects of heat generation, thermophoresis, and Brownian motion [26-31] are also taken into consideration. The governing equations are reduced to ODE by suitable similarity transformation and then solved numerically by using BVP4C from MATLAB. The effects of involved parameters on the distributions of velocity, temperature, concentration, and thin film thickness are presented graphically and discussed.

Problem formulation

Consider an unsteady flow and heat transfer of an upper convected Maxwell nanofluid in a finite thin liquid film over an unsteady stretching sheet. The fluid motion within the film is mainly on account of the stretching of the elastic sheet, as shown in fig. 1. It is assumed that the Maxwell nanofluid is incompressible and the flow is laminar.

The sheet emerges from a narrow slit at the origin of a Cartesian co-ordinate system. The continuous sheet moves with the velocity:

$$u_s = \frac{bx}{1-\mathrm{a}t} \tag{1}$$

where a and b are positive constants. It should be noted that the analysis is valid just for time $t < 1/a$. Let the concentration, C_s, at the sheet surface vary with the distance from the slit:

$$C_s = C_0 - C_{\mathrm{ref}} dx^2 (1-\mathrm{a}t)^{-3/2} \tag{2}$$

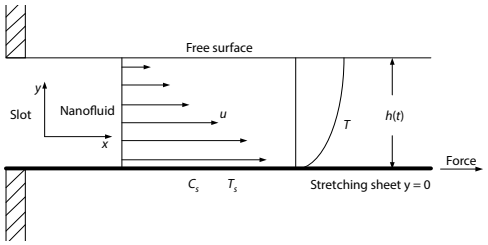

Figure 1. Schematic of the physical model

where C_0 is the concentration at the origin, d – the positive constant, C_{ref} – the reference concentration. The surface temperature, T_s, of the sheet varies with the distance x from the slot and time:

$$T_s = T_0 - T_{\mathrm{ref}} dx^2 (1-\mathrm{a}t)^{-3/2} \tag{3}$$

where T_0 denotes the temperature at the slot, T_{ref} – the positive reference temperature. The flow is governed by the continuity and momentum equations in the forms:

$$\nabla V = 0 \tag{4}$$

$$\rho e = \nabla B \tag{5}$$

in which V denotes the velocity vector and B is the Cauchy stress tensor. The acceleration vector e is defined:

$$e = \frac{\mathrm{d}V}{\mathrm{d}t} = \frac{\partial V}{\partial t} + (V\nabla)V \tag{6}$$

The Cauchy stress tensor in Maxwell fluid is given:

$$B = -pI + \mathrm{N} \tag{7}$$

in which an extra stress tensor N has the relation:

$$\left(1 + \lambda \frac{D}{Dt}\right)\mathrm{N} = \mu \mathrm{A}_1 \tag{8}$$

where λ is the relaxation time, μ – the dynamic viscosity, and the first Rivlin-Ericksen tensor A_1 can be expressed:

$$\mathrm{A}_1 = L + L^T \qquad L = \nabla V \tag{9}$$

For a two rank tensor N we have:

$$\frac{D\mathrm{N}}{Dt} = \frac{\partial \mathrm{N}}{\partial t} + (V\nabla)\mathrm{N} - L\mathrm{N} - \mathrm{N}L^T \tag{10}$$

Under these assumptions and Oberbeck-Boussinesq's approximation [26-31, 34], the governing equations for the model can be written:

$$\frac{\partial u}{\partial x} + \frac{\partial u}{\partial y} = 0 \tag{11}$$

$$\frac{\partial u}{\partial t} + u\frac{\partial u}{\partial x} + v\frac{\partial u}{\partial y} + \lambda\left(\begin{array}{l} \dfrac{\partial^2 u}{\partial t^2} + 2u\dfrac{\partial^2 u}{\partial x \partial t} + 2v\dfrac{\partial^2 u}{\partial y \partial t} + \\ +u^2\dfrac{\partial^2 u}{\partial x^2} + v^2\dfrac{\partial^2 u}{\partial y^2} + 2uv\dfrac{\partial^2 u}{\partial x \partial y} \end{array}\right) = \frac{\mu}{\rho}\frac{\partial^2 u}{\partial y^2} \tag{12}$$

$$\frac{\partial T}{\partial t}+u\frac{\partial T}{\partial x}+v\frac{\partial T}{\partial y}=\alpha\frac{\partial^2 T}{\partial y^2}+Q(t)+\tau\left[D_B\frac{\partial C}{\partial y}\frac{\partial T}{\partial y}+\frac{D_T}{T_0}\left(\frac{\partial T}{\partial y}\right)^2\right] \tag{13}$$

$$\frac{\partial C}{\partial t}+u\frac{\partial C}{\partial x}+v\frac{\partial C}{\partial y}=D_B\frac{\partial^2 C}{\partial y^2}+\frac{D_T}{T_0}\frac{\partial^2 T}{\partial y^2} \tag{14}$$

where u and v are the velocity components along the x- and y-direction, t – the time, μ – the dynamic viscosity, ρ – the density of the base fluid, $\lambda = \lambda_0(1- at)$ – the relaxation time, λ_0 is a constant, α – the thermal diffusivity of the base fluid, τ – the ratio of nanoparticle heat capacity and the base fluid heat capacity, C – the local concentration of the fluid, D_T – the Brownian diffusion coefficient, is the thermophoretic diffusion coefficient, the term $Q(t)$ is the heat generated or absorbed per unit volume which can be given by [34, 35]:

$$Q(t)=aQ_0\left(T-T_0\right)(1-at)^{-1} \tag{15}$$

The boundary conditions for the problem can be given by:

$$u=u_s,\quad v=0,\quad T=T_s,\quad C=C_s,\quad \text{at } y=0 \tag{16}$$

$$\frac{\partial u}{\partial y}=\frac{\partial T}{\partial y}=0,\qquad v=u\frac{\partial h}{\partial x}+\frac{\partial h}{\partial t}\qquad \frac{\partial C}{\partial y}=0,\ at\ \ y=h \tag{17}$$

where Q_0 is the internal heating parameter and $h(t)$ is the thin film thickness.

Numerical solutions

For the sake of simplifying investigation, we introduce dimensionless variables f, θ, ϕ, and the similarity variable η as:

$$\psi(x,y,t)=\left(\frac{bx^2\nu_f}{1-at}\right)^{1/2}f(\eta) \tag{18}$$

$$T=T_0-T_{\text{ref}}\frac{dx}{(\ at)^{3/2}}\theta(\eta) \tag{19}$$

$$C=C_0-C_{\text{ref}}\frac{dx}{(1\ \ \text{a})^{3/2}}\phi(\eta) \tag{20}$$

$$\eta=\left[\frac{b}{\nu_f(1-\text{at})}\right]^{1/2}y \tag{21}$$

$$\beta=\left[\frac{b}{\nu_f(1-\text{at})}\right]^{1/2}h(t) \tag{22}$$

where $\psi(x, y, t)$ is the stream function which is define by $u = \partial\psi/\partial y$ and $v = -\partial\psi/\partial x$, β – the dimensionless film thickness of the liquid film, $\nu_f = \mu/\rho$ – the kinematic viscosity.

According to these new variables, the governing eqs. (11)-(14) and the associated boundary conditions (16)-(17) are converted into:

$$f'''-S\left(f'+\frac{1}{2}f''\eta\right)-(f')^2+f''f-\text{De}\left[S^2\left(2f'+\frac{7}{4}f''\eta+\frac{1}{4}f'''\eta^2\right)\right]-$$
$$-\text{De}[S(2ff'+f''f'\eta-3f''f-f'''f\eta)+f^2f'''-2ff'f'']=0 \tag{23}$$

$$\frac{1}{\mathrm{Pr}}\theta'' + SQ_0\theta - Nb\theta'\phi' - Nt\theta'^2 + f\theta' - 2f'\theta - S\left(\frac{3}{2}\theta + \frac{1}{2}\theta'\eta\right) = 0 \tag{24}$$

$$\phi'' - \mathrm{Le}\left(2\phi f' - f\phi'\right) - \mathrm{Le}S\left(\frac{3}{2}\phi + \frac{1}{2}\phi'\eta\right) + \frac{Nt}{Nb}\theta'' = 0 \tag{25}$$

$$f'(0) = 1, \quad f(0) = 0, \quad \theta(0) = 1, \quad \phi(0) = 1 \tag{26}$$

$$\theta'(\beta) = 0, \quad \phi'(\beta) = 0, \quad f(\beta) = \frac{1}{2}\beta S, \quad f''(\beta) = 0 \tag{27}$$

where $S = a/b$ is the unsteadiness parameter, $\mathrm{De} = b\lambda_0$ – the Deborah number, $\mathrm{Pr} = \nu_f/\alpha$ – the Prandtl number, $\mathrm{Le} = \nu_f/D_b$ – the Lewis number, $Nb = [\tau D_B/\nu_f(C_0 - C_S)]$ – the Brownian number, $Nt = [\tau D_T/\nu_f T_0)(T_0 - T_s)]$ – the thermophesis parameter. According to [25-27, 34], the expressions for the local Nusselt number and local Sherwood number are given:

$$\frac{\mathrm{Nu}_x}{\sqrt{\mathrm{Re}_x}} = -\theta'(0) \quad \text{and} \quad \frac{\mathrm{Sh}_x}{\sqrt{\mathrm{Re}_x}} = -\phi'(0) \tag{28}$$

Following the literatures [25-27], the reduced local Nusselt number, Nu_r, and reduced local Sherwood number, Sh_r, can be introduced and presented:

$$\mathrm{Nu}_r = \frac{\mathrm{Nu}_x}{\sqrt{\mathrm{Re}_x}} = -\theta'(0) \quad \text{and} \quad \frac{\mathrm{Sh}_x}{\sqrt{\mathrm{Re}_x}} = -\phi(0) \tag{29}$$

where $\mathrm{Re}_x = u_s x/\nu_f$ is the local Reynolds number.

For solving the ODE (23)-(25) with the boundary conditions (26)-(27), we transform (23)-(25) to a system of first order differential equations. We denote f, f', f'', θ, θ', ϕ , and ϕ' variables by y_1, y_2, y_3, y_4, y_5, y_6, and y_7, respectively.

$$f = y_1 \tag{30}$$

$$f' = y_2 \tag{31}$$

$$f'' = \mathrm{y}_3 \tag{32}$$

$$f''' = \frac{\left\{S\left(f' + f''\frac{\eta}{2}\right) + (f')^2 - f''f + \mathrm{De}\left[S^2\left(2f' + \frac{7f''\eta}{4}\right)\right] - 2\,\mathrm{De}\,ff'f'' + \mathrm{De}S(2f'f' + f''f'\eta - 3ff'')\right\}}{\frac{1 - \mathrm{De}S^2\eta^2}{4 + \mathrm{De}f\eta - \mathrm{De}f^2}} \tag{33}$$

$$\theta = y_4 \tag{34}$$

$$\theta' = y_5 \tag{35}$$

$$\theta'' = y_5' = \mathrm{Pr}\left[Nby_5y_7 + Nty_5^2 - y_1y_5 + 2y_2y_4 + S\left(y_4 + \frac{1}{2}Sy_5\eta\right) - SQ_0y_4\right] \tag{36}$$

$$\phi = y_6 \tag{37}$$

$$\phi' = y_7 \tag{38}$$

$$\phi'' = y_7' = \mathrm{Le}(2y_6y_2 - y_1y_7) + \mathrm{Le}S\left(y_6 + \frac{1}{2}y_7\eta\right) - \frac{Nt}{Nb}y_5' \tag{39}$$

$$y_2(0) = 1, \quad y_1(0) = 0, \quad y_4(0) = 1, \quad y_6(0) = 1 \tag{40}$$

$$y_3(\beta)=0,\quad y_5(\beta)=0,\quad y_7(\beta)=0,\quad y_1(\beta)=\frac{1}{2}\beta S \tag{41}$$

In order to obtain the numerical solutions, we use the program Bvp4c in MATLAB to solve the seven ODE (31)-(33), (35)-(36), and (38)-(39) with eight boundary conditions (40)-(41). There exists a certain relationship between β and S from the boundary condition $y_1(\beta)=\beta S/2$.

Results and discussion

In this section, the numerical solutions of eqs. (23)-(27) are obtained by the program Bvp4c. To verify the accuracy and effectiveness of this method, present results are compared with some of the earlier published results in tab. 1. It is noteworthy that the present numerical solutions are in very good agreement.

Table 1. Comparison of the dimensionless film thickness β and friction coefficient $f''(0)$ for De = 0

S	Wang [5]		Abel *et al.* [8]		Present results	
	β	$f''(0)$	β	$f''(0)$	β	$f''(0)$
0.4	5.122490	–6.699120	4.981455	–1.134098	4.981454	–1.134096
0.6	3.131250	–3.742330	3.131710	–1.195128	3.131710	–1.195125
0.8	2.151990	–2.680940	2.151990	–1.245805	2.151993	–1.245805
1.0	1.543620	–1.972380	1.543617	–1.277769	1.543616	–1.277769
1.2	1.127780	–1.442631	1.127780	–1.279171	1.127780	–1.279171
1.4	0.821032	–1.012784	0.821033	–1.233545	0.821032	–1.233544
1.6	0.576173	–0.642397	0.576176	–1.114941	0.576173	–1.11493764

Figures. 2-4 show the distribution of the dimensionless velocity, temperature, and nanoparticle volume fraction with different values of Deborah number, respectively. It is clear that the thin film thickness increases as Deborah number increases. As shown in fig. 2, the velocity boundary-layer becomes lager with the increase of Deborah number. It is found that both the velocity and thin film thickness increase with the increases (increasing value of Deborah number) of elastic force of the fluid. The free-surface velocity arrives at its minimum value for De = 0, which showing that the internal elastic force of fluid disappears, the fluid becomes a Newtonian fluid. Figure 3 show that the boundary-layer thickness of temperature and nanoparticle volume fraction decreases with the increase of Deborah number. Figure 4 indicates that the nanoparticle volume fraction increases at first, arriving at a maximum, and then it decreases with η increases. It illustrates that the viscoelastic relaxation framework system has strongly effects on thermal and concentration transmission.

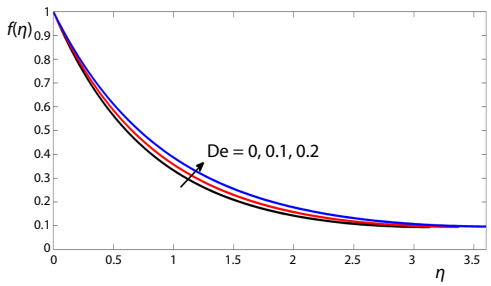

Figure 2. Variations of the velocity $f'(\eta)$ with different values of De for S = 0.6, Le = 3, Pr = 1, Nb = 0.2, Nt = 0.8, and Q_0 = 0.5

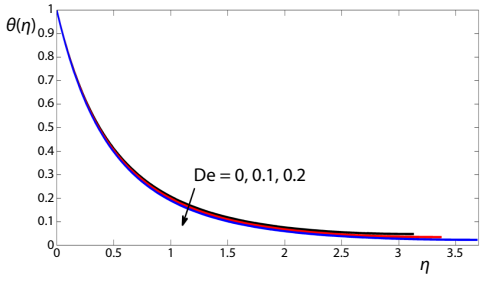

Figure 3. Variations of the temperature $\theta(\eta)$ with different values of De for S = 0.6, Le = 3, Pr = 1, Nb = 0.2, Nt = 0.8, and Q_0 = 0.5

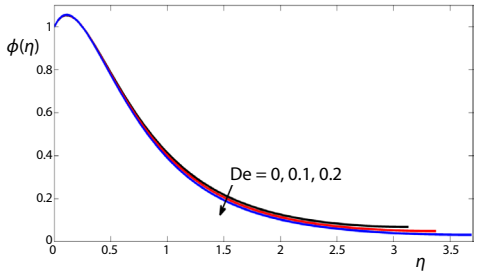

Figure 4. Variations of nanoparticle volume fraction $\phi(\eta)$ with different values of De for $S = 0.6$, Le = 3, Pr = 1, $Nb = 0.2$, $Nt = 0.8$, and $Q_0 = 0.5$

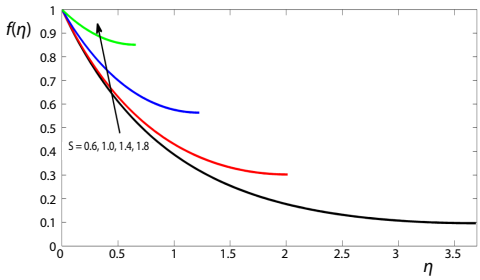

Figure 5. Variations of the velocity $f'(\eta)$ with different values of S for De = 0.2, Le = 3, Pr = 1, $Nb = 0.2$, $Nt = 0.8$, and $Q_0 = 0.5$

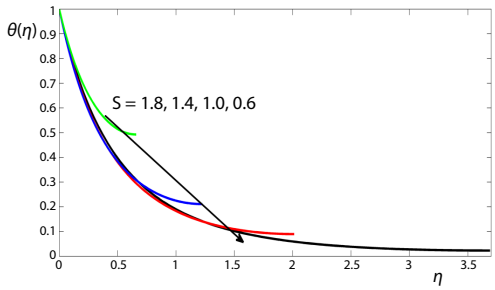

Figure 6. Variations of the temperature $\theta(\eta)$ with different values of S for De = 0.2, Le = 3, Pr = 1, $Nb = 0.2$, $Nt = 0.8$, and $Q_0 = 0.5$

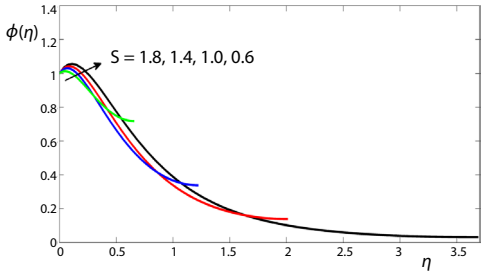

Figure 7. Variations of nanoparticle volume fraction $\phi(\eta)$ with different values of S for De = 0.2, Le = 3, Pr = 1, $Nb = 0.2$, $Nt = 0.8$, and $Q_0 = 0.5$

Figures 5-7 display effects of the unsteady parameter on the velocity, temperature and nanoparticle volume fraction, respectively. The velocity boundary-layer decreases with the decrease of S. There exists intersections in the temperature and nanoparticle volume fraction profiles with the relaxation effects (De $\neq$ 0) for different values of S which is different from the based fluid of Newtonian (De = 0) [34]. It implies that the unsteady parameter has a critical influence on the thermal and concentration transmission.

The variations in the nanoparticle volume fraction with different values of Q_0 are shown in fig. 8. It is illustrated that the nanoparticle volume fraction decreases with the increase of Q_0. Figure 9 indicates the effects of S on the nanofluid film thickness with different values of Deborah number. The nanofluid film thickness decreases with S increases from 0.4-1.9. When $S \to 0$ as seen in fig. 9, it represents the liquid film thickness of an infinitely thickness ($\beta \to \infty$).

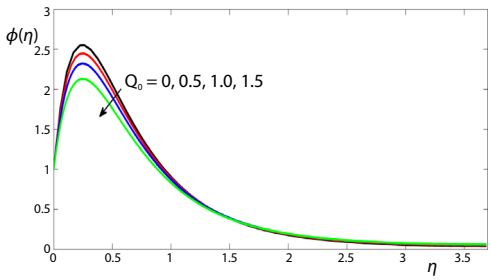

Figure 8. Variations of nanoparticle volume fraction $\phi(\eta)$ with different values of Q_0 for De = 0.2, Le = 3, Pr = 1, $Nb = 0.2$, $Nt = 0.8$, and $S = 0.6$

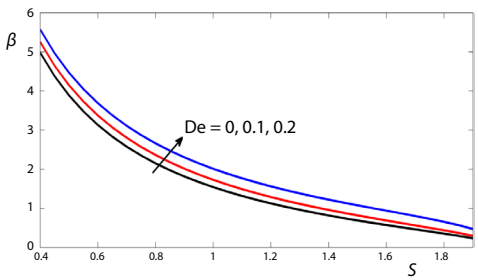

Figure 9. Variations of the film thickness β with S for different values of De for Le = 3, Pr = 1, $Nb = 0.2$, $Nt = 0.8$, and $Q_0 = 0.6$

For the particular value S_0 of S no solutions can be obtained. While $S \to S_0$ it stands for the case of an infinitesimal thick fluid layer ($\beta \to 0$).

Figures 10 and 11 show the variations of the reduced local Nusselt number and Sherwood number with different values of Deborah number *vs*. increasing S, respectively. Figure 10 displays that the reduced local Nusselt number increases at first, and then decreases with S increases for different values of Deborah number. It shows that the rate of heat transfer is more evident with the effect of unsteady parameter. Moreover, the rate of heat transfer increases with the viscoelastic relaxation Deborah number increases. As seen in fig. 11, the reduced local Sherwood number increases with the increase of S for different of Deborah number. It implies that the increase of unsteady parameter leads to the enhancement of concentration transfer of nanoparticle.

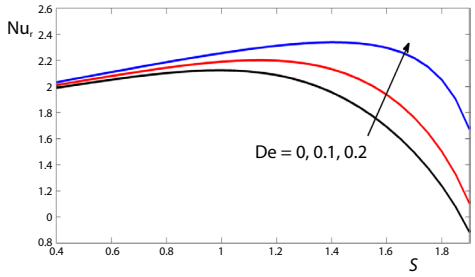

Figure 10. The reduced Nusselt number Nu_R with S for different values of De for Le = 3, Pr = 1, Nb = 0.2, Nt = 0.8, and Q_0 = 0.5

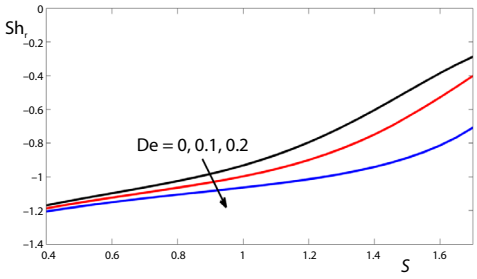

Figure 11. The reduced Sherwood number Sh_r with S or different values of De for Le = 3, Pr = 1, Nb = 0.2, Nt = 0.8, and Q_0 = 0.5

Figures 12 and 13 present the distribution of the reduced local Nusselt number and Sherwood number with different values of *Nb vs*. increasing *Nt*, respectively. It can be seen from fig. 12 that the rate of heat transfer increases with the increasing thermophoresis parameter and Brownian motion parameter. Figure 13 indicates that the concentration transfer of nanoparticle decreases with the thermophoresis parameter increases, while it increases with the increasing Brownian motion parameter.

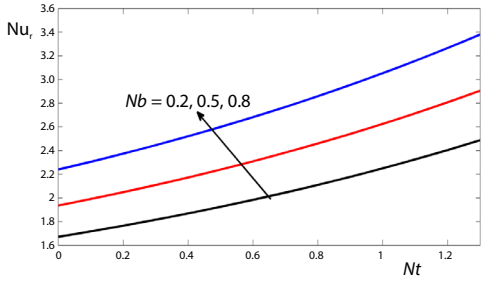

Figure 12. The reduced Nusselt number Nu_r with Nt for different values of Nb on condition that De = 0.2, Le = 3, Pr = 1, S = 0.6, and Q_0 = 0.5

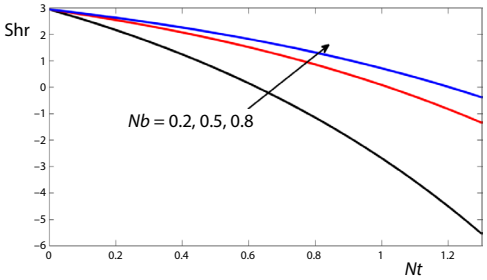

Figure 13. The educed Sherwood number Sh_r with Nt for different values of Nb on condition that De = 0.2, Le = 3, Pr = 1, S = 0.6, and Q_0 = 0.5

Conclusions

The flow and heat transfer of Maxwell nanofluid in a finite thin film over an unsteady stretching sheet with internal heat generation or absorption are studied. Meanwhile, the effects of Brownian motion and thermophoresis are considered. The problem is strongly non-linear.

For simplicity, local similarity solutions are obtained by using the method of similarity transformation. Further research about the experiments should be done to verify the accuracy and reliability of the numerical results. The influence of the involved parameters on the velocity, temperature, nanoparticle volume fraction and thin film thickness are analyzed. What we have obtained can be summarized as follows.

- The Deborah number tends to increase the velocity boundary-layer and increase the thermal and concentration transmission of the fluid. The thin film thickness also increases with the increase of the Deborah number.
- The thin film thickness decreases with the increase of the unsteady parameter. There exists intersections in the temperature and nanoparticle volume fraction profiles with the relaxation effects for different values of *S*. It implies that the unsteady parameter has a critical influence on the thermal and concentration transmission.
- The rate of heat transfer increases at first, and then decreases as the unsteady parameter increases. The concentration transfer of nanoparticle increases with the increase of the unsteady parameter.
- The rate of heat transfer increases with the increasing thermophoresis parameter and Brownian motion parameter. The concentration transfer of nanoparticle decreases with the thermophoresis parameter increases, while it increases with the increasing Brownian motion parameter.

Acknowledgment

The work is supported by the National Natural Science Foundation of China (No. 51276014, 11772046).

Nomenclature

a – constant, [s^{-1}]
b – stretching rate, [s^{-1}]
C – nanoparticle fraction, [–]
C_0, C_{ref} – nanoparticle fraction constant, [–]
D_B – Brownian diffusion coefficient, [–]
D_T – thermophoretic diffusion coefficient, [–]
De – Deborah number, [–]
d – constant, [–]
f – dimensionless stream function, [–]
h – film thickness, [m]
Le – Lewis number, [–]
Nb – Brownian motion parameter, [–]
Nt – thermophoresis parameter, [–]
Nu_r – reduced local Nusselt number, [–]
Nu_x – local Nusselt number, [–]
Pr – Prandtl number, [–]
Q – heat generated or absorbed per unit volume, [–]
Q_0 – internal heating parameter, [–]
Re_x – local Reynolds number, [–]
S – unsteadyness parameter, [–]
Sh_r – reduced local Sherwood number, [–]
Sh_x – local Sherwood number, [–]
T – temperature, [K]
T_0, T_{ref} – temperature constant, [K]
t – time, [s]
u – horizontal velocity component, [ms^{-1}]
u_s – sheet velocity, [ms^{-1}]
v – vertical velocity component, [ms^{-1}]
x – horizontal co-ordinate, [m][
y – vertical co-ordinate, [m]

Greek symbols

α – thermal diffusivity, [m^2s^{-1}]
β – dimensionless film thickness, [–]
η – similarity variable, [–]
θ – dimensionless temperature, [–]
μ – dynamic viscosity, [$kgm^{-1}s^{-1}$]
ν – kinametic viscosity, [m^2s^{-1}]
ρ – density, [kgm^{-3}]
τ – ratio between the effective heat capacity of the nanoparticle material and heat capacity of the fluid, [–]
ϕ – rescaled nanoparticle volume fraction. [–]
ψ – stream function, [–]

References

[1] Crane, L. J., Flow Past a Stretching Plate, *Z. Angrew. Math. Phys.*, *21* (1970), 4, pp. 645-647

[2] Wang , C. Y., Liquid Film on an Unsteady Stretching Surface, *Q. Appl. Math*., *48* (1990), 4, pp. 601-610
[3] Andersson, I., *et al.*, Flow of a Power-Law Fluid Film on Unsteady Stretching Surface, *Journal Non-Newtonian Fluid Mech*., *62* (1996), 1, pp. 1-8
[4] Chen, C., Heat Transfer in a Power-Law Fuid Film over an Unsteady Stretching Sheet, *Heat and Mass Transfer*, *39* (2003), 8-9, pp. 791-796
[5] Wang, C., Analytic Solutions for a Liquid Film on an Unsteady Stretching Surface, *Heat Mass Transfer*, *42* (2006), 8, pp. 759-766
[6] Dandapat, B. S., *et al*., The Effects of Variable Fluid Properties and Thermocapillarity on the Flow of a Thin Film on an Unsteady Stretching Sheet, *Int. J. Heat Mass Transfer*, *50* (2007), 5-6, pp. 991-996
[7] Chen, C., Marangoni Effects on Forced Convection of Power-Law Liquids in a Thin Film over a Stretching Surface, *Physics Letters A*, *370* (2007), 1, pp. 51-57
[8] Abel, M. S., *et al*., Heat Transfer in a Liquid Film over an Unsteady Stretching Surface with Viscous Dissipation in Presence of External Magnetic Field, *Applied Mathematical Modelling*, *33* (2009), 8, pp. 3430-3441
[9] Abbas, Z. *et al*., MHD Boundary-Layer Flow of an Upper-Convected Maxwell Fluid in a Porous Channel, *Theor. Comput. Fluid Dyn*., *20* (2006), 4, pp. 229-238
[10] Abbas, Z., *et al*. Unsteady Flow of a Second Grade Fluid Film over an Unsteady Stretching Sheet, *Mathematical and Computer Modelling*, *48* (2008), 3-4, pp. 518-526
[11] Hayat, T., *et al*., MHD Flow and Mass Transfer of a Upper-Convected Maxwell Fluid Past a Porous Shrinking Sheet with Chemical Reaction Species, *Physics Letters A*, *372* (2008), 26, pp. 4698-4704
[12] Sajid, M., *et al*., Unsteady Flow and Heat Transfer of a Second Grade Fluid over a Stretching Sheet, *Commun. Nonlinear Sci. Numer. Simulat.*, *14* (2009), 1, pp. 96-108
[13] Alizadeh-Pahlavan, A., Sadeghy, K., On the Use of Homotopy Analysis Method for Solving Unsteady MHD Flow of Maxwellian Fluids above Impulsively Stretching Sheets, *Commun. Nonlinear Sci..Numer*. *Simulat*., *14* (2009), 4, pp. 13551365
[14] Aliakbar, V., *et al*., The Influence of Thermal Radiation on MHD Flow of Maxwellian Fluids above Stretching Sheets, *Commun. Nonlinear Sci. Numer. Simulat*., *14* (2009), 3, pp. 779-794
[15] Hayat, T., *et al*., Mass Transfer Effects on the Unsteady Flow of UCM Fluid over a Stretching Sheet, *Int*. *J. Mod. Phys*. *– B*, *25* (2011), 21, pp. 2863-2878
[16] Awais, M., *et al*., Time-Dependent Three-Dimensional Boundary-Layer Flow of a Maxwell Fluid, *Computers & Fluids*, *91* (2014), Mar., pp. 21-27
[17] Hsiao, K., Combined Electrical MHD Heat Transfer Thermal Extrusion System Using Maxwell Fluid with Radiative and Viscous Disspation Effects, *Applied Thermal Engineering*, *112* (2017), Feb., pp. 1281-1288
[18] Kumaran, G., *et al*., Computational Analysis of Magnetohydrodynamic Casson and Maxwell Flows over a Stretching Sheet with Cross Diffusion, *Results in Physics*, *7* (2016), Dec., pp. 147-155
[19] Hayat, T., *et al*., Three-Dimensional Rotating Flow of Maxwell Nanofluid, *Journal of Molecular Liquids*, 229 (2017), Mar., pp. 495-500
[20] Hayat, T., *et al*., An Optimal Study for Three-Dimensional Flow of Maxwell Nanofluid Subject to Rotating Frame, *Journal of Molecular Liquids*, *229* (2017), Mar., pp. 541-547
[21] Choi, S., Enhancing Thermal Conductivity of Fluids with Nanoparticles, *Develop. Appl. Non-Newtonian Flows*, *66* (1995), Jan., pp. 99-105
[22] Pak, B. C., Cho, Y., Hydrodynamic and Heat Transfer Study of Dispersed Fluids with Submicron Metallic Oxide Particles, *Exp. Heat Transfer*, *11* (1998), 2, pp. 151-170
[23] Das, S., Temperature Dependence of Thermal Conductivity Enhancement for Nanofluids, *J. Heat Transfer*, *125* (2003), 4, pp. 567-574
[24] Minsta, H. A., *et al.*, New Temperature Dependent Thermal Conductivity Data for Water-Based Nanofluids, *Int. J. Thermal Science, 48* (2009), 2, pp. 363-371
[25] Khan, W. A., Pop, I., Boundary-Layer Flow of a Nanofluid Past a Stretching Sheet, *Int. J. Heat Mass Transfer*, *53* (2010), 11-12, pp. 2477-2483
[26] Kuznetsov, A. V., Nield, D. A., Natural Convective Boundary Flow of a Nanofluid Past a Vertical Plate, *Int. J. Thermal Science*, *49* (2010), 2, pp. 243-247
[27] Khan, W. A., Aziz, A., Natural Convection Flow of a Nanofluid over a Vertical Plate with Uniform Surface Heat Flux*, Int. J. Thermal Science*, *50* (2011), 7, pp. 1207-1214
[28] Pakravan, H. A., Yaghoubi, M., Combined Thermophoresis, Brownian Motion and Dufour Effects on Natural Convection of Nanofluids, *Int. J. Thermal Science*, *50* (2011), 3, pp. 394-402
[29] Bachok, N., *et al*., Unsteady Boundary-Layer Flow and Heat Transfer of a Nanofluid over a Permeable Stretching/Shrinking Sheet, *Int. J. Heat Mass Transfer*, *55* (2012), 7-8, pp. 2102-2109

[30] Hamad, M. A. A., Ferdows, M., Similarity Solution of Boundary-Layer Stagnation-Point Flow Towards a Heated Porous Stretching Sheet Saturated with a Nanofluid with Heat Absorption /Generation and Suction /Blowing: A Lie Group Analysis, *Commun. Nonlinear Sci. Numer Simulat*., *17* (2012), 1, pp. 132-140
[31] Zheng, L. C., *et al*., Flow and Radiation Heat Transfer of a Nanofluid over a Stretching Sheet with Velocity Slip and Temperature Jump in Porous Medium, *Journal of the Franklin Institute*, *350* (2013), 5, pp. 990-1007
[32] Shehzad, S. A., *et al*., Thermophoresis Particle Deposition in Mixed Convection Three-Dimensional Radiative Flow of an Oldroyd-B Fluid, *Journal of the Taiwan Institute of Chemical Engineers*, *45* (2014), 3, pp. 787-794
[33] Lin, Y. H., *et al*., MHD Pseudo-Plastic Nanofluid Unsteady Flow and Heat Transfer in a Finite Thin Film over Stretching Surface with Internal Heat Generation, *Int. J. Heat Mass Transfer*, *84* (2015), May, pp. 903-911
[34] Li, J., *et al*., Unsteady MHD Flow and Radiation Heat Transfer of Nanofluid in a Finite Thin Film with Heat Generation and Thermophoresis, *Journal of the Taiwan Institute of Chemical Engineers*, *64* (2016), Oct., pp. 226-234
[35] Hayat, T., *et al*., Magnetohydrodynamic Three-Dimensional Flow of Viscoelastic Nanofluid in the Presence of Nonlinear Thermal Radiation, *Journal of Magnetism and Magnetic Materials*, *385* (2015), July, pp. 222-229
[36] De, P., *et al*., Dual Solutions of Heat and Mass Transfer of Nanofluid over a Stretching/Shrinking Sheet with Thermal Radiation, *Meccanica*, *51* (2016), 1, pp. 117-124
[37] Bhatti, M. M., *et al*., A Mathematical Model of MHD Nanofluid Flow Having Gyrotactic Microorganisms with Thermal Radiation and Chemical Reaction Effects, *Neural Computing and Applications*, *30* (2016), 4, pp. 1237-1249
[38] Bhatti, M. M., *et al*., Entropy Analysis on Titanium Magneto-Nanoparticles Suspended in Water-Based Nanofluid: A Numerical Study, *Computational Thermal Sciences*, *8* (2016), 5, pp. 457-468
[39] Ayub, M., *et al*., Inspiration of Slip Effects on Electromagnetohydrodynamics (EMHD) Nanofluid Flow through a Horizontal Riga Plate, *The European Physical Journal Plus*, *131* (2016), 6, 193
[40] Abbas, T., *et al*., Entropy Generation on Nanofluid Flow through a Horizontal Riga Plate, *Entropy*, *18* (2016), 6, 223
[41] Hayat, T. *et al*., Flow of Nanofluid Due to Convectively Heated Riga Plate with Variable Thickness, *Tounal of Molecular Liquids*, *222* (2016), Oct., pp. 854-862
[42] Hayat, T., *et al*., On Magnetohydrodynamic Three-Dimensional Flow of Nanofluid over a Convectively Heated Nonlinear Stretching Surface, *International Journal of Heat and Mass Transfer*, *100* (2016) Sept., pp. 566-572
[43] Hayat, T., *et al*., On Magnetohydrodynamic Flow of Nanofluid Due to a Rotating Disk with Slip Effect: A Numerical Study, *Comput. Methods Appl. Mech. Engrg.*, *315* (2017), Mar., pp. 467-477

Paper submitted: January 29, 2017
Paper revised: March 22, 2017
Paper accepted: March 24, 2017